NASA Contractor Report 165843

NASA-CR-165843
19850021606

APPLICATION OF AN AERODYNAMIC ANALYSIS METHOD INCLUDING ATTAINABLE THRUST ESTIMATES TO LOW SPEED LEADING-EDGE FLAP DESIGN FOR SUPERSONIC CRUISE VEHICLES

Harry W. Carlson

KENTRON INTERNATIONAL, INC.
Hampton Technical Center
an LTV company
Hampton, Virginia 23666

Contract NAS1-16000
March 1982

NASA
National Aeronautics and
Space Administration

Langley Research Center
Hampton, Virginia 23665

SUMMARY

A study of low speed leading-edge flap design for supersonic cruise vehicles has been conducted. Wings with flaps were analyzed with the aid of a newly developed subsonic wing program which provides estimates of attainable leading-edge thrust. Results indicate that the thrust actually attainable can have a significant influence on the design and that the resultant flaps can be smaller and simpler than those resulting from more conventional approaches.

INTRODUCTION

The highly-swept low-aspect-ratio wings which permit high levels of aerodynamic efficiency at supersonic cruise conditions present serious problems in the low speed flight regime. One of these problems is the achievement of a sufficiently high lift coefficient to permit safe terminal area speed at an angle of attack which does not limit pilot visibility. The required lift coefficients can be generated at acceptable angles of attack through use of trailing-edge flaps. Unfortunately, for conventional supersonic cruise designs with wing-mounted engines and outboard ailerons, only a small portion of the trailing-edge span may be used for this purpose. Thus, large flap deflections are required to generate the additional lift, and drag penalties may be excessive. Properly designed leading-edge flaps can bring about significant improvements in the aerodynamic efficiency without reduction of the lift coefficient or increase in the associated angle of attack.

As reported in reference 1, significant progress has been made in improvement of the aerodynamic efficiency of leading- and trailing-edge flaps for supersonic cruise configurations. The conventional approach to leading-edge flap design has been to place segmented flaps on all of the wing area ahead of the front wing spar and to conduct wind-tunnel tests to determine optimum deflections.

A somewhat different approach to the leading-edge flap design problem is the subject of this paper. The concept is based on the observation that the primary purpose of the flap system is the achievement of an aerodynamic efficiency comparable to that which could be attained with full theoretical leading edge thrust. Accordingly, the new approach first attempts to assertain the local degree of achievement of leading edge thrust for the basic wing. Then, as required in a design by iteration process, local geometry changes in the form of leading edge flaps to compensate for the loss of thrust are introduced. Thus, for portions of the wing leading-edge where full theoretical thrust may be anticipated no flaps need be employed, and for the remainder of the leading-edge the flap chord and deflection angles may be limited to values just sufficient to restore the efficiency losses due to the failure to develop full leading-edge thrust.

The use of the computer program of reference 2 in the estimation of attainable leading-edge thrust and in the prediction of the aerodynamic characteristics of flap configurations is shown in comparisons with experimental data for a generic supersonic transport model. Further application of the computer program in an iterative design mode is illustrated in a sample problem - the definition of flap geometry for a typical supersonic transport in landing approach.

SYMBOLS

AR	wing aspect ratio, b^2/S
b	wing span
c_A	section axial force coefficient
c_N	section normal force coefficient
c_T	section thrust coefficient
c_D	section drag coefficient
c_L	section lift coefficient
C_A	axial force coefficient
C_N	normal force coefficient
C_D	drag coefficient
C_L	lift coefficient
C_{L_α}	lift curve slope, $dC_L/d\alpha$
L_1, L_2	designation of leading-edge flaps
T_1, T_2	designation of trailing-edge flaps
M	Mach number
y	lateral distance from wing centerline
s	suction parameter, $\dfrac{C_L \tan (C_L/C_{L_\alpha}) - C_D}{C_L \tan (C_L/C_{L_\alpha}) - C_L^2/(\pi AR)}$
S	wing reference area
R	Reynolds number
α	angle of attack
δ_L	leading-edge flap deflection angle, positive for leading-edge down
δ_T	trailing-edge flap deflection angle, positive for trailing edge down
ϵ_L	local angle of wing surface at the leading-edge relative to the free stream direction, includes basic wing camber and leading-edge flap deflection

Subscripts

n measured in a plane perpendicular to the hinge line

s measured in a plane parallel to the free stream

DISCUSSION

Assessment of Computer Program Applicability

The computer program of reference 2 which provides estimates of attainable thrust for wings at subsonic speeds is based on a planar solution of linearized theory equations. To study the applicability of the program to the present problem, comparisons of program results with previously unpublished data from tests conducted in the Langley Research Center V/STOL Tunnel have been made, and are shown in figure 1. The wind-tunnel model employed in these tests is particularly appropriate for this purpose. It represents a M = 2.7 cruise vehicle, but for simplicity only the wing and fuselage are represented in the model and the wing has no twist and camber. The low speed test conditions are $M \approx .28$ and $R \approx 5.7 \times 10^6$. The program has inherent limitations in the accuracy of flap planform modeling due to the wing element grid system employed. Although the spanwise position of the flap edges could only be approximated, the flap areas were matched by compensating changes in the flap chord.

In figure 1(a), the program results are compared with data for the basic flat wing. There is good agreement between the theory and experiment for the full range of angles of attack and lift coefficients. The axial force correlation is particularly significant since it shows an appreciable degree of achievement of leading-edge thrust. The normal force curve shows evidence of the presence of vortex lift, which is also accurately estimated by the program.

Figures 1(b) to 1(d) show similar correlations for a series of leading-edge flap deflections with the trailing-edge flap deflection fixed at 10°. Both trailing-edge flaps [see sketch in figure 1(a)] were set at 10°. The correlations are not as good as for the undeflected case, but there is still a reasonably good prediction of the lift-drag polar.

Figures 1(e) to 1(g) show correlations for a series of trailing-edge deflections with leading-edge flap deflections maintained at 30°. For this 30° leading-edge flap deflection, axial and normal force predictions are poor. There are, however, compensating effects so that the lift-drag relationships are given reasonably well in the $C_L = .4$ to $C_L = .8$ range. The program is seen to underestimate the amount of leading edge thrust and overestimate the normal force.

The ability of the program to assess trends may be examined with the aid of figure 2. Here data from figure 1 is shown as a function of leading edge and trailing edge deflection angles. The suction parameter s is defined as in reference 1 to be a measure of drag relative to the limits for fully attached and fully separated flow. These results indicate that, despite some inaccuracies in the absolute values predicted, the program may be used in a design process.

The Design Problem

The configuration of Table I has been taken as an example for application of various flap designs (see reference 3 for an explanation of the format used for the geometric description given in Table I). This is a wing-fuselage-vertical tail configuration with a twisted and cambered wing designed for $C_L = 0.10$ at $M = 2.7$. Landing approach design conditions have been chosen as:

$$M = .25$$
$$R = 160 \times 10^6$$
$$C_L = .55$$
$$\alpha = 8°$$

Two trailing-edge flaps on either side of the airplane (between the fuselage and the inboard engine, and between the inboard and the outboard engine) are fixed in planform but may be deflected as necessary (the same angle for both). It is assumed that trailing-edge devices for the remainder of the wing will be employed as ailerons for roll control and will be unavailable for use in generating lift.

Conventional Design Approach

As a base-line reference, conventional leading-edge flaps similar to those treated in reference 1 have been analyzed. In that reference the test results indicated that a uniform deflection along the entire leading-edge performed as well as, if not better than, any other deflection schedule included in the tests. Accordingly, the conventional flap analysis will be simplified by the assumption of a constant deflection over the whole of the leading-edge. Results of the analysis are summarized in figure 3. The simplification of one deflection angle for the trailing-edge flaps and one deflection angle for the leading-edge flaps permits the program results to be presented in the form of a contour map. Suction parameters at $C_L = .55$ and angles of attack corresponding to $C_L = .55$ are shown by the contour lines as a function of the leading- and trailing-edge deflection angles.

According to the map, the optimum performance of the flap configuration subject to the limitation of $\alpha \leq 8°$ occurs for a trailing-edge flap deflection of about 20° and a leading-edge deflection of about 13° (when measured normal to the hinge line this angle is about 34° for the inboard wing panel and about 22° for the outer panel). The indicated suction parameter is about 0.70. Based on the previous correlations of experiment and theory, it is likely that a somehwat higher suction parameter could be realized (perhaps as high as 0.78). However, it also is likely that a larger trailing-edge flap deflection would be required to generate a lift coefficient of .55 at $\alpha = 8°$. This contour map also indicates that misleading results could be obtained if the variation of suction parameter with leading-edge deflection angle were examined at a trailing-edge flap deflection angle (say $\delta_T = 0°$) other than that for optimum performance.

Design Approach Based On Attainable Thrust

To initiate the new design for the present configuration, the program of reference 2 was used to estimate the spanwise distribution of forces on the wing basic camber surface as shown in figure 4. For the design lift coefficient of

0.55, full theoretical thrust is estimated for the inboard 20 percent of the wing semispan. The loss in thrust beyond that point is felt as an increase in normal force according to the Polhamus Suction Analogy.

At the design conditions, the inboard portion of the wing leading-edge is more likely to perform as it does at 8° angle of attack than as it does at a lift coefficient of 0.55. The additional lift generated by the trailing-edge flaps can have little influence on the leading-edge. Figure 5 shows program data for the 8° angle of attack design condition. Here full leading-edge thrust is seen to extend to 25 percent or more of the wing semispan.

Based on the preceeding information, a leading-edge flap design was developed and subjected to program evaluation. The results are shown on the suction parameter contour map of figure 6. An inset sketch shows the selected flap system planform. The flap chord increases linearly from 0 percent of the local chord at y/b/2 = .25 to 36 percent of the local chord at the leading-edge break. From there it decreases linearly to 30 percent of the chord of the wing tip. Both flap segments L_1 and L_2 are simply hinged and are deflected to the same angle relative to the freestream direction.

The program results presented in figure 6 show a modest gain in suction parameter over the reference design (s = 0.74 compared to 0.70), and the new design is simpler and could probably be constructed with less weight penalty. The leading-edge flap deflection for optimum performance is quite large, about 35° (64° and 50° respectively for the inboard and outboard panel when measured normal to the hinge line). It is quite possible that the true optimum condition would be reached at a considerably smaller deflection angle. The program results do indicate no great sensitivity of the suction parameter to leading-edge deflection when the $\alpha \leq 8°$ restriction is imposed. As with the more conventional design previously discussed, it is likely that the actual suction parameter would be somewhat higher and that the required trailing-edge flap deflection would be greater.

The design conditions for this example were a lift coefficient of .55, a Mach number of .25, and a full scale Reynolds number of 160 X 10^6. For another set of design conditions it would be necessary to redefine the flap geometry and prepare a new suction parameter contour map. In general, a lower design lift coefficient would permit a more outboard origin of the flap and smaller flap deflection angles, and a higher design lift coefficient would have the opposite effect. Lower design Mach numbers and higher design Reynolds numbers favor the development of thrust and thus would lead to smaller leading-edge flap systems.

The dependence of attainable thrust on both Mach number and Reynolds number complicates the problem of extrapolation of tunnel test results to full scale conditions. For example, if tests of this flap system were made at a Mach number of .2 and a Reynolds number of 3.5 X 10^6, an extrapolation to full scale design conditions would indicate no appreciable improvement in aerodynamic performance. A discussion of extrapolation to account for leading-edge thrust effects is given in reference 2.

Program aerodynamic forces for the partial span leading-edge flap arrangement are shown in figure 7. The peculiar nature of the axial force curves (the no thrust and full thrust curves do not meet) is due to the distinct regions of the wing leading-edge. Inboard of the flaps, the angle of attack for zero thrust is between -2 and -3 degrees. On the flaps, the angle of attack for zero thrust is between 6 and 8 degrees. Thus, some thrust is produced at all angles of attack.

Note also that little or no vortex lift is developed at the design condition, as should be the case if the flap serves to maintain attached flow.

The spanwise distribution of forces on the wing with partial span leading-edge flaps at the design condition is shown in figure 8. The most obvious changes from the basic camber surface distribution (figures 4 and 5) are in the axial force distribution where the drag penalties of the deflected trailing-edge flaps appear to dominate. However, there is also a large region of the wing outboard of the mid-semispan where a significant thrusting force has been realized. This is due to the leading-edge flap operating in the large upwash field generated by the forward part of the wing. This benefit is similar to that which could be achieved were it possible for the full theoretical thrust to be developed.

The partial span leading-edge flap design based on attainable thrust considerations employs a constant deflection angle for the entire length of the flap. Figure 9 was prepared as a means of judging possible improvements with other deflection schedules. Section drag due-to-lift factors have been plotted as a function of the leading-edge flap deflection. To eliminate the intermingling of curves that otherwise would occur, the drag due-to-lift factors shown are increments relative to the zero leading-edge deflection values. For the outer half of the wing semispan, minimum section drag due-to-lift factors generally occur in the 35° to 40° deflection range. This data thus indicates that other deflection schedules would offer little or no benefit over the constant deflection angle. The linearly increasing flap chord probably results in an effective leading-edge camber which matches the increasing upwash field. As additional evidence, several other deflection schedules were evaluated by use of the program. None of these offered any improvements.

Comparison of Flap Designs

In addition to the basic camber surface alone and the two flap designs just discussed, several other variations of these designs were evaluated. The results are depicted in figure 10. Suction parameters at a C_L of .55 are shown for eight configurations. For the flat wing, an angle of attack of 13.1° was required to generate the design lift coefficient. For this wing with no camber and no flaps, the suction parameter was 0.49. The wing with a camber surface designed for supersonic cruise, had a significant improvement in suction parameter to 0.59 and achieved the design lift coefficient at an angle of attack of 10.5°.

The remainder of the configurations of figure 10 employed trailing-edge flaps which permitted the design goals of $C_L = .55$ and $\alpha = 8°$ to be achieved simultaneously. The conventional design approach discussed previously, yielded a further improvement in suction parameter to almost 0.70. The next configuration differed from the conventional design only in the elimination of the inboard leading-edge flap. It is interesting to note that the present analysis shows a slight improvement in suction factor. The fifth configuraion is the result of the design approach based on attainable thrust. This design, already discussed in detail, has a program predicted suction factor of 0.74.

The last three configurations employ leading-edge flaps with parabolic streamwise curvature. The deflection is proportional to the square of the distance forward of the hinge line. Data for the sixth configuration indicates a further substantial increase in suction parameter to a little more than .80. Actual benefits of this more sophisticated system would depend on the weight penalties of the more complicated actuator system. Because of the strong influence of the outer flap panel in reduction of the overall drag (refer to figure 9 for example), one configuration with a double area outboard flap was examined. As shown, this produced a negligible improvement. The final configuration was included to indicate the penalties being paid for the severe restrictions imposed on the span of the two trailing-edge flaps. Program results indicates that if the trailing-edge flap could extend over the entire wing span, a suction parameter of 0.86 could be achieved. It was somewhat surprising that a larger difference was not indicated.

Based on correlations of computer program results with experimental data for a wing-body of similar planform (see figure 2) it is anticipated that somehwat better suction parameters than shown in figure 10 could be achieved in practice.

CONCLUSIONS

A study of low speed leading-edge flap design for supersonic cruise vehicles, based on a recently developed computer program with attainable thrust estimates, indicates the following conclusions:

(1) Leading-edge flaps are not required and, in fact, are undesirable at span stations where full leading-edge thrust is attainable. For the example treated this includes the inboard 25 percent of the wing semispan.

(2) Outboard of the station where thrust loss begins, a linearly increasing flap chord appears to produce the effect of increasing camber and eliminate the need for flap segmenting. A simple design with a constant deflection about the hinge line is thus acceptable.

(3) Leading-edge flaps with camber surface curvature are preferable from an aerodynamic standpoint but do, of course, create other design problems.

REFERENCES

1. Coe, Paul L.; Thomas, James L.; Huffman, Jarrett K.; Weston, Robert P.; Schoonover, Ward E. Jr.; and Gentry, Carl L. Jr.: Overview of the Langley Subsonic Research Effort on SCR Configurations. Supersonic Cruise Research '79, Part 1. Proceedings of a conference held at Langley Research Center, Hampton, Virginia, November 13-16, 1979. NASA Conference Publication 2108. Paper 1.

2. Carlson, Harry W.; and Walkley, Kenneth B.: A Computer Program for Wing Subsonic Aerodynamic Performance Estimates Including Attainable Thrust and Vortex Lift Effects. NASA CR-3515, 1982.

3. Craidon, Charlotte B.: Description of a Digital Computer Program for Airplane Configuration Plots. NASA TM X-2074, 1970.

Table I. - Wind Tunnel Model Definition (inches).

SCR LOW-SPEED GENERIC MODEL (6/19/80) WBF

1 1 -1 1 20 20 1 19 24 1 10

1335.5335.465 65.309										REFS
0.000	.500	1.000	1.500	2.500	5.000	10.000	15.000	20.000	30.000	XAF 10
40.000	50.000	60.000	70.000	75.000	80.000	85.000	90.000	95.000	100.000	XAF 20
20.858	0.000	7.089	65.908							WORG 1
22.889	.620	6.458	63.865							WORG 2
24.919	1.240	5.880	61.821							WORG 3
28.718	2.400	4.801	57.998							WORGT1-1
33.041	3.720	3.675	53.647							WORG 5
37.103	4.960	2.755	49.561							WORG 6
41.164	6.200	1.999	45.474							WORG 7
44.013	7.070	1.584	42.606							WORGT1-2
47.976	8.280	1.134	38.618							WORG 8
52.102	9.540	0.774	34.836							WORGT2-1
56.760	10.962	0.477	30.569							WORGT2-M
61.273	12.340	0.257	26.431							WORGT2-2
65.426	13.606	0.210	22.624							WORG 11
69.984	15.000	0.198	19.309							WORGT3-1
73.653	16.120	0.153	16.646							WORG 13
79.810	18.000	0.117	12.162							WORGT3-2
79.810	18.001	0.117	12.162							WORGT4-1
82.997	19.840	0.123	10.589							WORG 16
87.292	22.320	0.118	8.470							WORG 17
91.588	24.800	0.079	6.350							WORGT4-2
0.000	-.010	-.020	-.030	-.049	-.132	-.428	-.837	-1.312	-2.357	TZ 1.1
-3.400	-4.355	-5.194	-5.915	-6.236	-6.530	-6.801	-7.045	-7.258	-7.429	TZ 1.2
0.000	-.009	-.019	-.027	-.045	-.137	-.425	-.801	-1.233	-2.166	TZ 2.1
-3.092	-3.942	-4.695	-5.353	-5.652	-5.930	-6.189	-6.426	-6.637	-6.812	TZ 2.2
0.000	-.005	-.011	-.016	-.034	-.124	-.394	-.742	-1.136	-1.978	TZ 3.1
-2.807	-3.569	-4.249	-4.853	-5.130	-5.390	-5.634	-5.860	-6.064	-6.236	TZ 3.2
0.000	-.004	-.009	-.013	-.023	-.082	-.296	-.577	-.893	-1.563	TZ-T1.1
-2.222	-2.835	-3.395	-3.907	-4.147	-4.377	-4.597	-4.809	-4.997	-5.165	TZ-T1.2
0.000	.002	.004	.006	.002	-.027	-.175	-.375	-.605	-1.094	TZ 5.1
-1.584	-2.052	-2.494	-2.916	-3.121	-3.323	-3.519	-3.709	-3.888	-4.052	TZ 5.2
0.000	.005	.009	.014	.023	.014	-.069	-.206	-.362	-.707	TZ 6.1
-1.064	-1.418	-1.768	-2.117	-2.292	-2.468	-2.643	-2.814	-2.981	-3.137	TZ 6.2
0.000	.005	.011	.016	.027	.054	.015	-.062	-.161	-.392	TZ 7.1
-.644	-.909	-1.184	-1.473	-1.622	-1.774	-1.928	-2.082	-2.234	-2.380	TZ 7.2
0.	.008	.015	.024	.039	.060	.047	0.	-.069	-.237	TZ-T1.1
-.434	-.649	-.883	-1.134	-1.267	-1.403	-1.542	-1.683	-1.825	-1.961	TZ-T1.2
0.000	.008	.017	.026	.043	.077	.090	.073	.035	-.071	TZ 8.1
-.210	-.373	-.563	-.774	-.889	-1.007	-1.130	-1.255	-1.381	-1.506	TZ 8.2
0.000	.008	.016	.024	.041	.075	.109	.113	.097	.033	TZ-T2.1
-.065	-.192	-.344	-.522	-.619	-.721	-.826	-.935	-1.045	-1.155	TZ-T2.2
0.	.008	.016	.024	.040	.079	.116	.131	.130	.095	TZ-TM.1
.027	-.069	-.190	-.333	-.413	-.496	-.583	-.692	-.763	-.855	TZ-TM.2
0.000	.006	.014	.020	.033	.067	.117	.140	.149	.129	TZ-T2.1
.079	.006	-.091	-.205	-.269	-.336	-.406	-.479	-.553	-.626	TZ-T2.2
0.000	.006	.013	.019	.032	.064	.102	.125	.137	.131	TZ11.1
.098	.038	-.039	-.132	-.185	-.240	-.298	-.358	-.417	-.479	TZ11.2
0	.005	.010	.015	.025	.050	.094	.113	.123	.117	TZ-T3.1
.098	.040	-.023	-.097	-.137	-.179	-.223	-.269	-.314	-.359	TZ-T3.2
0.000	.004	.007	.011	.019	.038	.070	.098	.104	.101	TZ13.1
.074	.034	-.020	-.083	-.116	-.150	-.183	-.218	-.252	-.285	TZ13.2
0.000	.001	.002	.003	.005	.009	.019	.020	.021	.011	TZ-T3.1
-.010	-.036	-.065	-.097	-.113	-.129	-.144	-.158	-.173	-.188	TZ-T3.2
0.000	.001	.002	.003	.005	.009	.019	.020	.021	.011	TZ-T4.1
-.010	-.036	-.065	-.097	-.113	-.129	-.144	-.158	-.173	-.188	TZ-T4.2

Table I. - Concluded.

0.000	-.002	-.003	-.004	-.008	-.015	-.027	-.033	-.039	-.053	TZ16.1
-.069	-.083	-.100	-.116	-.122	-.129	-.134	-.138	-.144	-.148	TZ16.2
0.000	-.001	-.004	-.005	-.009	-.018	-.037	-.053	-.062	-.079	TZ17.1
-.094	-.108	-.114	-.120	-.118	-.118	-.116	-.114	-.112	-.110	TZ17.2
0.000	-.001	-.002	-.002	-.005	-.010	-.018	-.028	-.037	-.055	TZ-T4.1
-.066	-.075	-.078	-.079	-.079	-.079	-.078	-.078	-.078	-.078	TZ-T4.2
0.	.242	.339	.413	.521	.726	.996	1.181	1.318	1.490	WORD1.1
1.543	1.543	1.543	1.213	1.021	.819	.615	.413	.212	0.	WORD1.2
0.	.242	.339	.413	.521	.726	.996	1.181	1.318	1.490	WORD2.1
1.543	1.543	1.543	1.213	1.021	.819	.615	.413	.212	0.	WORD2.2
0.	.242	.339	.413	.521	.726	.996	1.181	1.318	1.490	WORD3.1
1.543	1.543	1.543	1.213	1.021	.819	.615	.413	.212	0.	WORD3.2
0.000	.237	.333	.406	.514	.713	.979	1.159	1.294	1.463	WORDT1-1
1.514	1.514	1.514	1.193	1.004	.807	.607	.405	.208	0.000	WORDT1-1
0.000	.225	.316	.386	.490	.679	.931	1.103	1.232	1.392	WORD5.1
1.441	1.441	1.437	1.132	.953	.765	.576	.385	.197	0.000	WORD5.2
0.000	.216	.304	.370	.470	.651	.894	1.059	1.182	1.336	WORD6.1
1.383	1.383	1.341	1.056	.889	.714	.537	.360	.184	0.000	WORD6.2
0.000	.208	.294	.358	.455	.631	.866	1.025	1.144	1.293	WORD7.1
1.338	1.338	1.277	1.006	.848	.681	.512	.343	.175	0.000	WORD7.2
0.	.205	.289	.352	.449	.621	.852	1.009	1.126	1.273	WORDT1-2
1.317	1.317	1.239	.976	.823	.661	.497	.333	.170	0.	WORDT1-2
0.000	.200	.283	.344	.438	.607	.833	.987	1.101	1.244	WORD8.1
1.297	1.287	1.186	.935	.788	.633	.476	.319	.163	0.000	WORD8.2
0.000	.198	.281	.342	.436	.603	.828	.981	1.094	1.236	WORDT2-1
1.279	1.279	1.167	.920	.775	.622	.468	.314	.160	0.000	WORDT2-1
0.000	.204	.288	.350	.445	.616	.846	1.002	1.119	1.264	WORDT2-2
1.308	1.308	1.154	.910	.766	.616	.463	.310	.157	0.000	WORDT2-2
0.	.200	.282	.343	.438	.606	.832	.985	1.099	1.242	WORDTM
1.286	1.286	1.154	.910	.766	.616	.463	.310	.157	0.000	WORDTM
0.000	.209	.295	.359	.457	.632	.868	1.028	1.148	1.297	WORD11.1
1.342	1.342	1.164	.917	.773	.621	.467	.313	.160	0.000	WORD11.2
0.000	.217	.305	.371	.471	.653	.897	1.062	1.184	1.339	WORDT3-1
1.386	1.386	1.201	.948	.798	.641	.482	.323	.164	0.000	WORDT3-1
0.000	.222	.313	.381	.484	.670	.920	1.090	1.216	1.375	WORD13.1
1.423	1.423	1.234	.972	.819	.659	.495	.331	.169	0.000	WORD13.2
0.000	.235	.330	.402	.510	.706	.969	1.148	1.282	1.449	WORDT3-2
1.500	1.500	1.300	1.024	.862	.692	.521	.349	.178	0.000	WORDT3-2
0.000	.029	.059	.088	.146	.285	.541	.766	.961	1.261	WORDT4-1
1.440	1.500	1.440	1.261	1.126	.961	.766	.541	.285	0.000	WORDT4-1
0.000	.029	.059	.088	.146	.285	.541	.766	.961	1.261	WORD16.1
1.440	1.500	1.440	1.261	1.126	.961	.766	.541	.285	0.000	WORD16.2
0.000	.029	.059	.088	.146	.285	.541	.766	.961	1.261	WORD17.1
1.440	1.500	1.440	1.261	1.126	.961	.766	.541	.285	0.000	WORD17.2
0.000	.029	.059	.088	.146	.285	.541	.766	.961	1.261	WORDT4-2
1.440	1.500	1.440	1.261	1.126	.961	.766	.541	.285	0.000	WORDT4-2
0.	3.911	7.821	11.733	15.644	19.555	23.466	27.377	31.287	35.198	XFUS 10
39.109	43.020	46.931	50.842	54.753	58.664	62.575	66.486	70.397	74.308	XFUS 20
78.219	82.130	86.040	86.766							XFUS 30
8.390	8.370	8.340	8.280	8.190	8.040	7.835	7.490	7.008	6.492	ZFUS 10
5.907	5.344	4.770	4.286	3.791	3.369	2.968	2.594	2.232	1.902	ZFUS 20
1.596	1.314	1.059	1.020							ZFUS 30
0.	1.086	3.028	5.430	8.305	11.624	14.852	16.366	16.947	16.366	AFUS 10
15.173	15.127	15.387	15.754	16.244	16.871	17.620	18.094	18.156	18.354	AFUS 20
18.324	18.156	17.437	17.250							AFUS 30
79.810	18.000	0.117	13.752	92.806	18.000	3.987	1.872			V FIN
0.	10.	20.	30.	40.	50.	60.	70.	90.	100.	XFIN
0.	.466	.846	1.138	1.345	1.465	1.498	1.390	.641	0.	FINORD

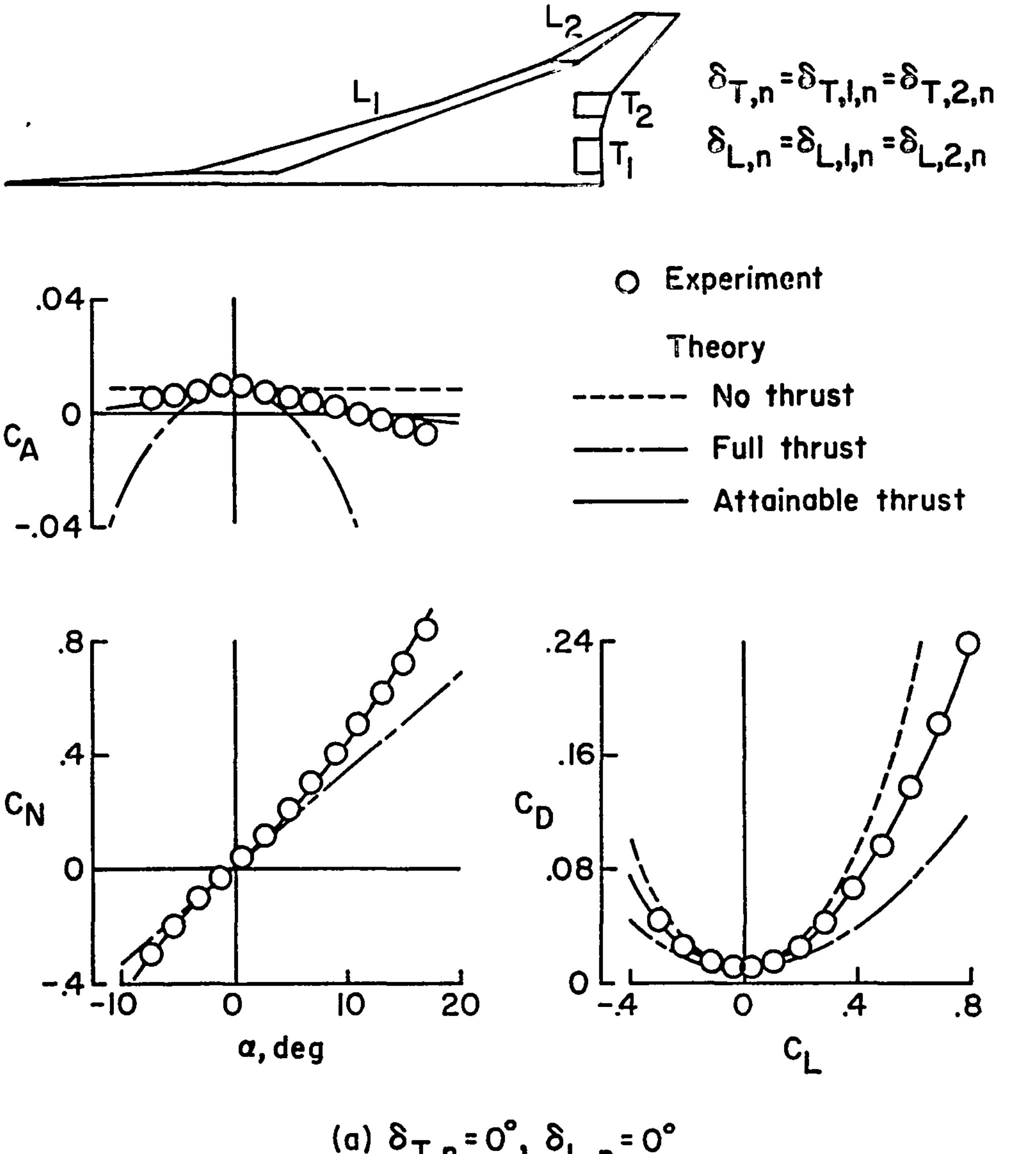

(a) $\delta_{T,n} = 0°$, $\delta_{L,n} = 0°$

Figure 1. - Correlation of program data with experimental data.
M = .28. R = 5.75 x 10^6

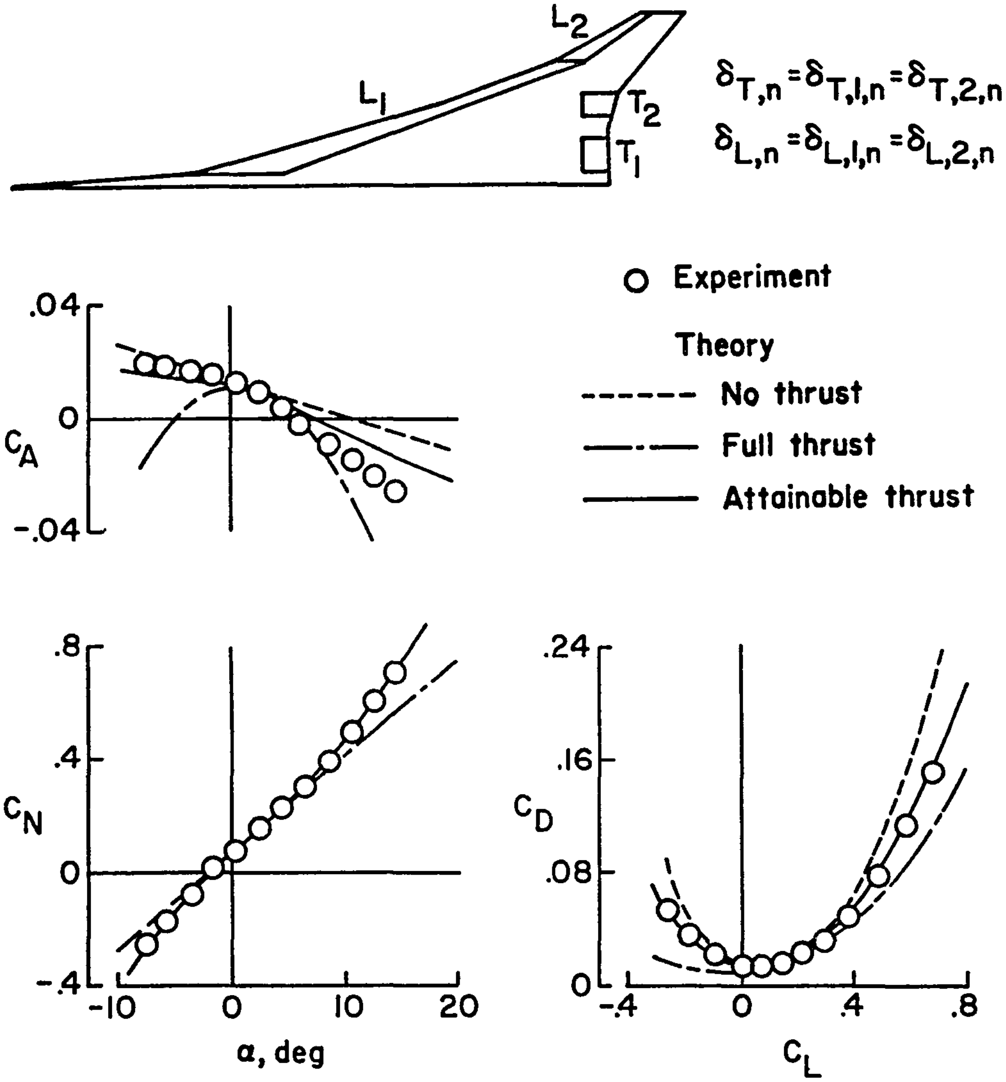

(b) $\delta_{T,n} = 10°$, $\delta_{L,n} = 20°$

Figure 1. - Continued

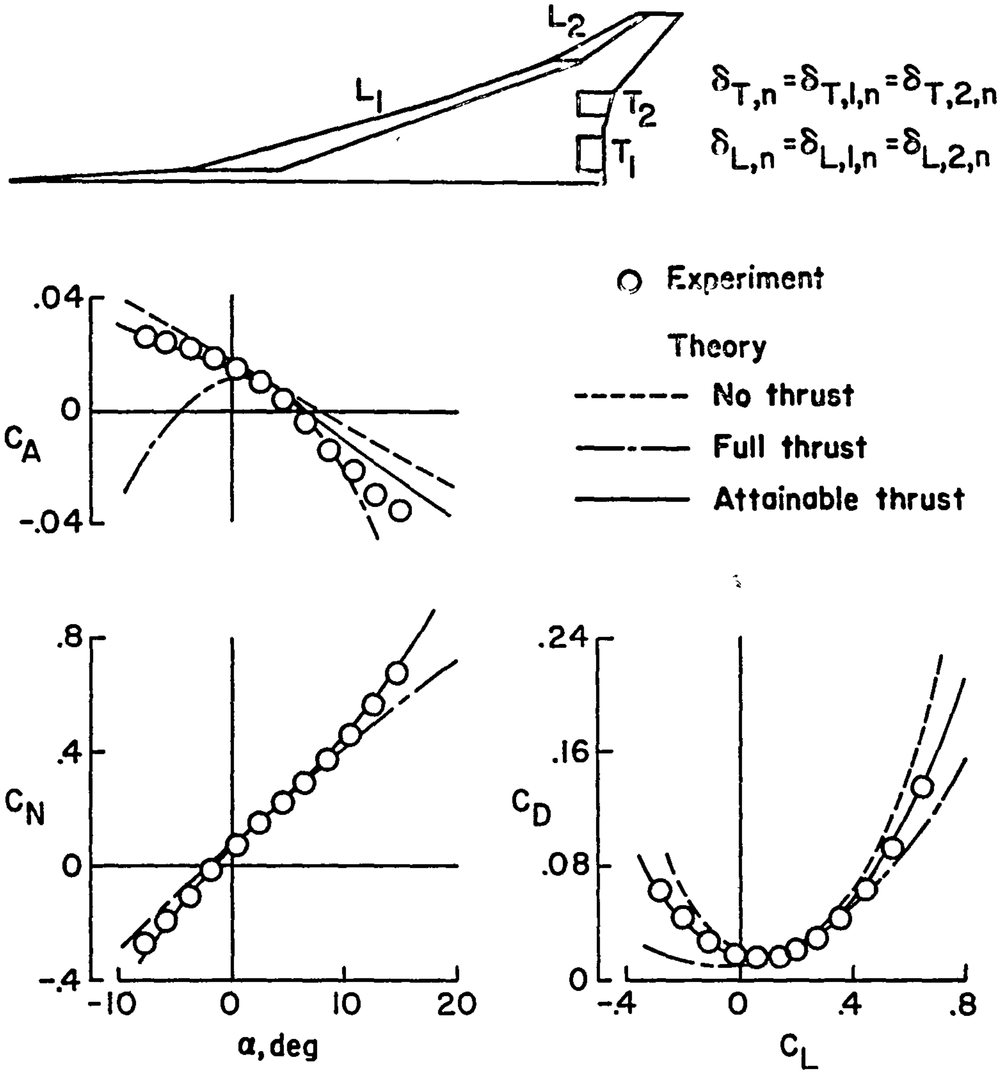

(c) $\delta_{T,n} = 10°$, $\delta_{L,n} = 30°$

Figure 1. - Continued

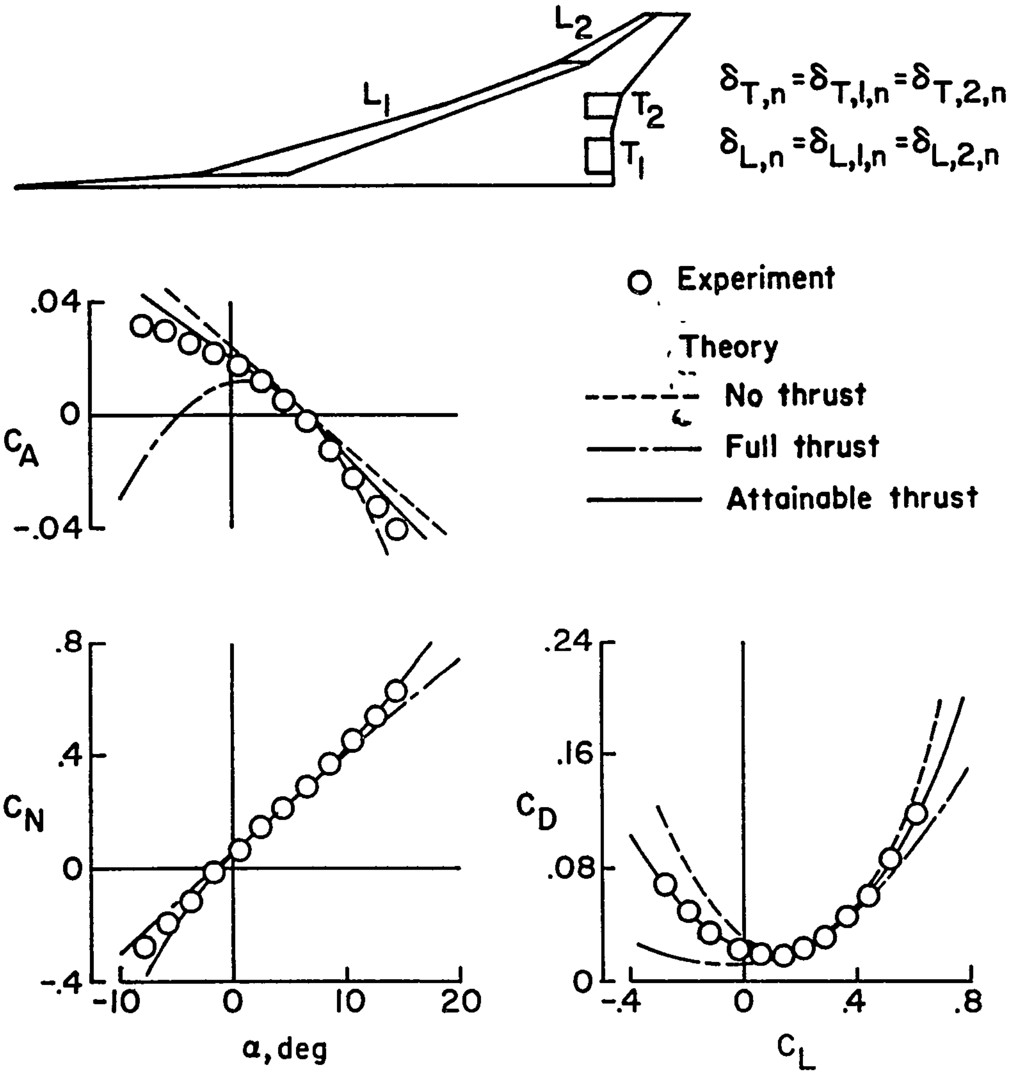

(d) $\delta_{T,n} = 10°$, $\delta_{L,n} = 40°$

Figure 1. - Continued

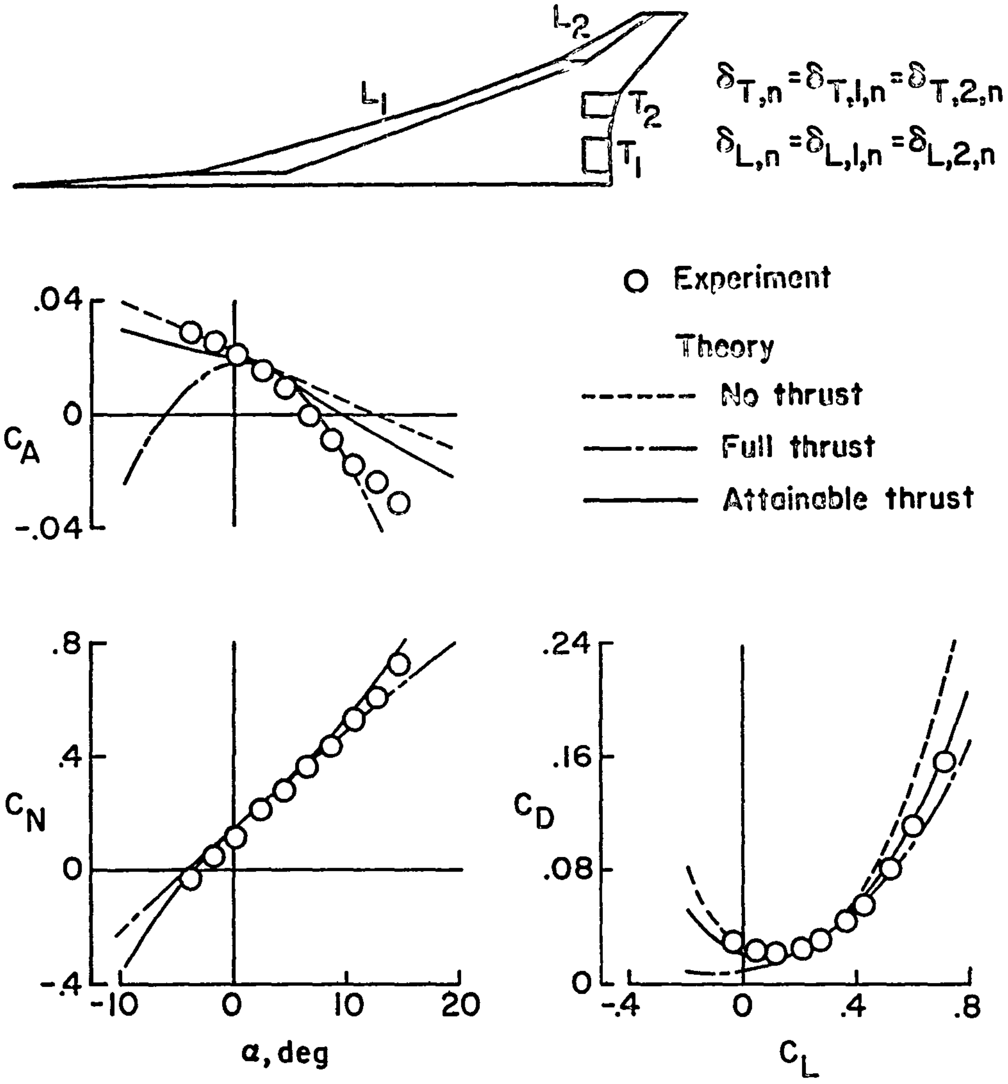

(e) $\delta_{T,n} = 20°, \delta_{L,n} = 30°$

Figure 1. - Continued

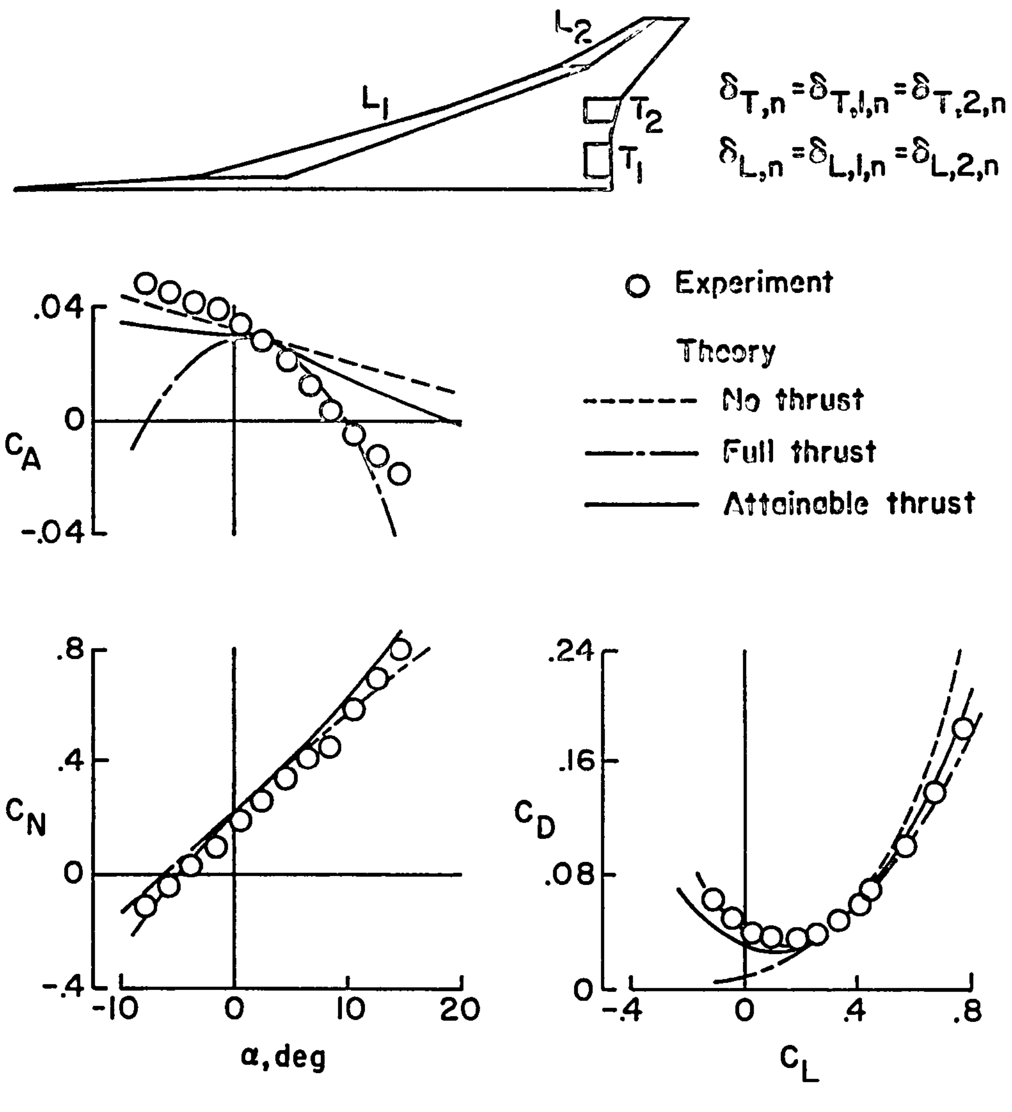

(f) $\delta_{T,n} = 30°$, $\delta_{L,n} = 30°$

Figure 1. - Continued

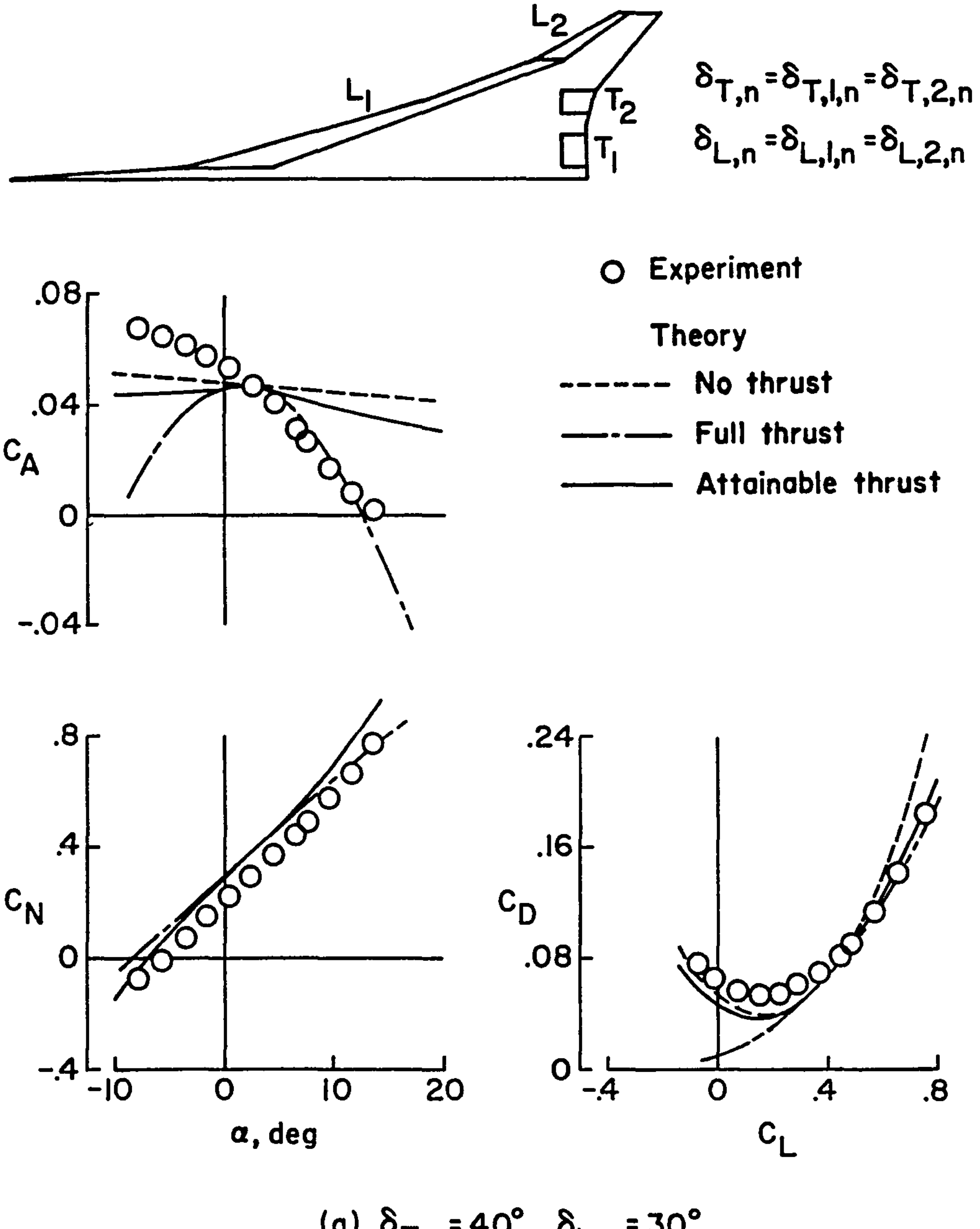

(g) $\delta_{T,n} = 40°$, $\delta_{L,n} = 30°$

Figure 1. - Concluded

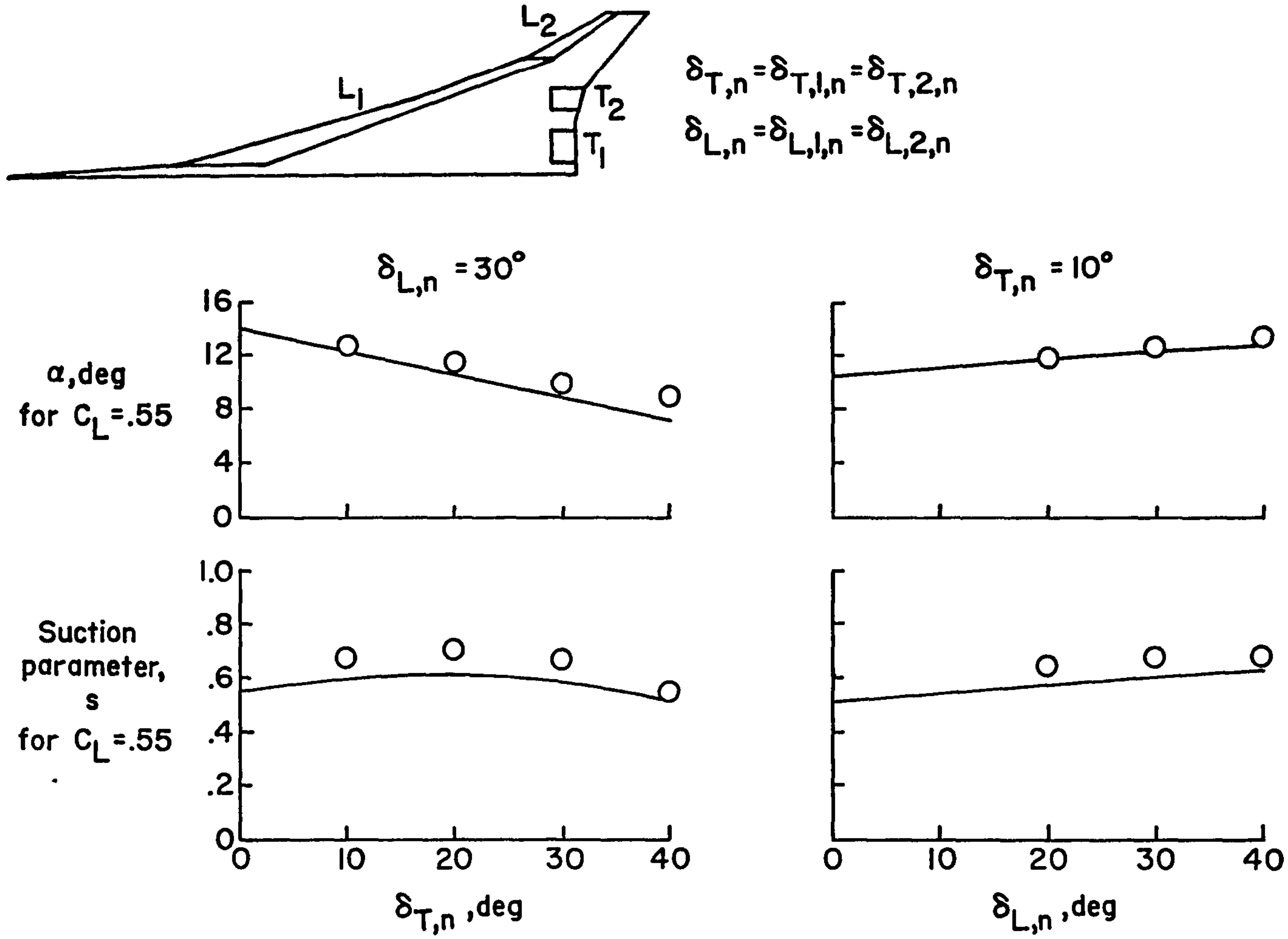

Figure 2. - Comparison of program suction parameters with experimental data.
$M = .28.\quad R = 5.75 \times 10^6$

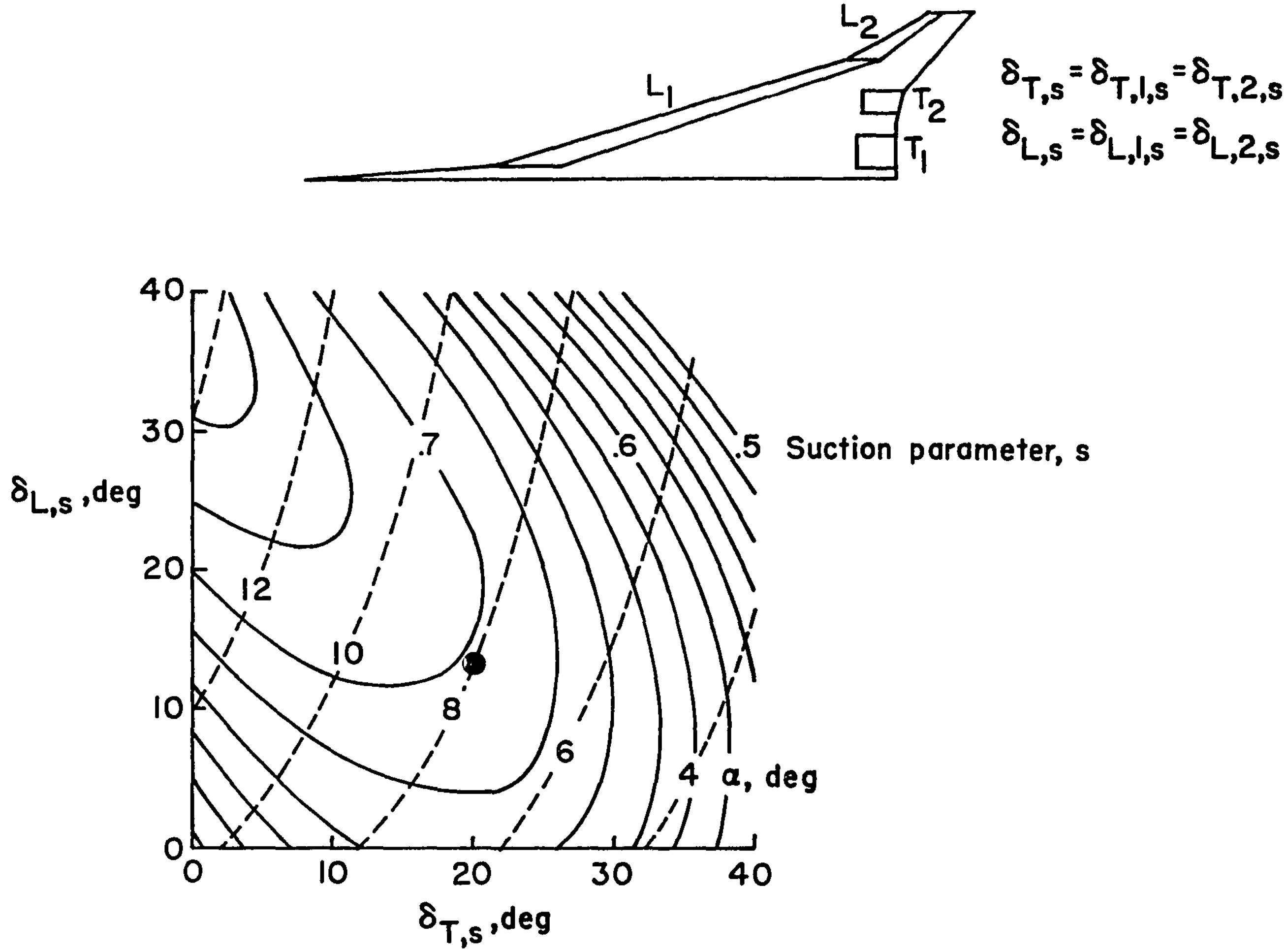

Figure 3. - Suction parameters and angles of attack at C_L = .55 for full span leading edge flap system.

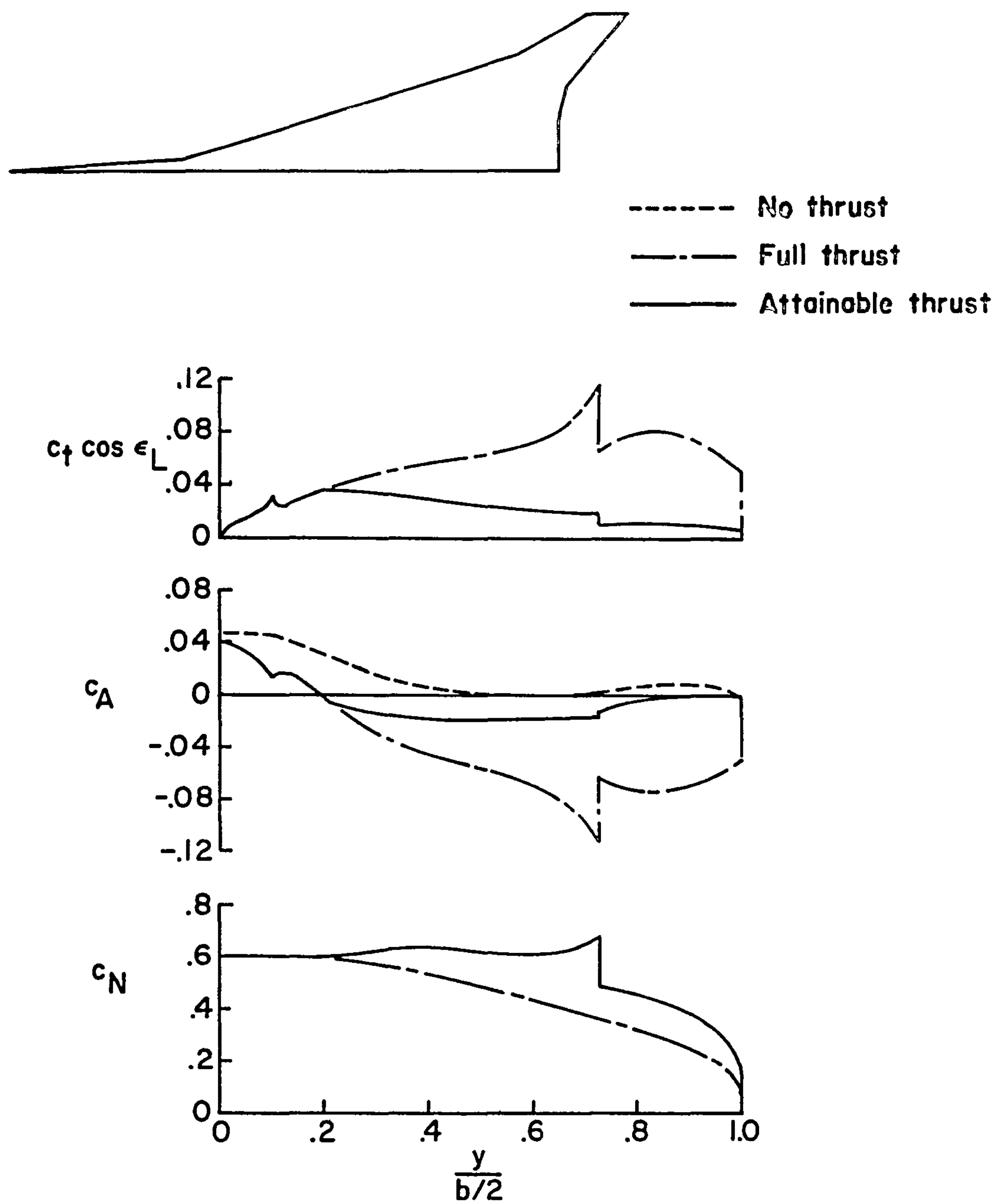

Figure 4. - Spanwise distribution of forces on the basic camber surface at the design lift coefficient. C_L = .55. α = 10.48°.

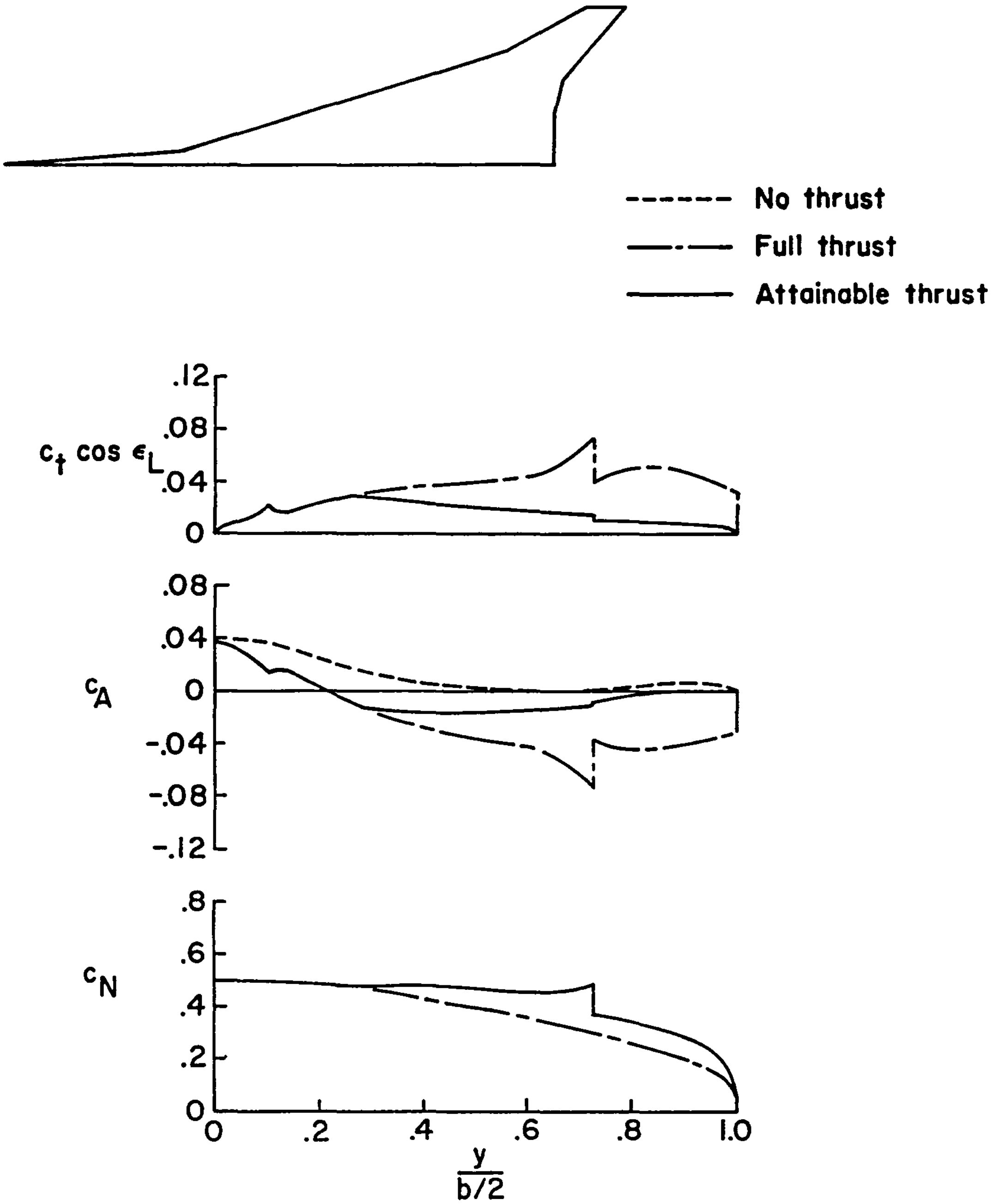

Figure 5. - Spanwise distribution of forces on the basic camber surface at the design angle of attack. $\alpha = 8°$. $C_L = .425$.

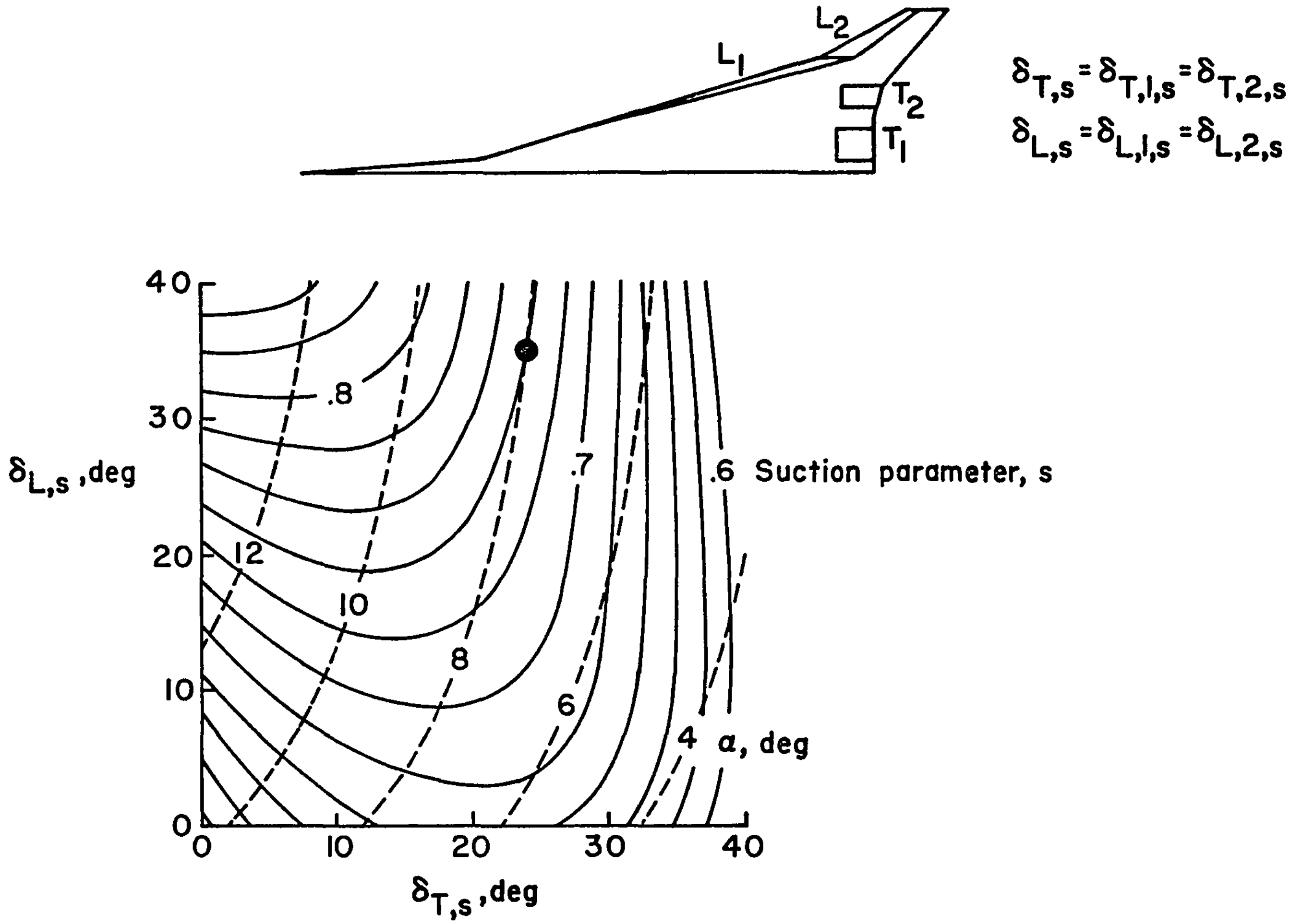

Figure 6. - Suction parameters and angles of attack at C_L = .55 for partial span leading edge flap system.

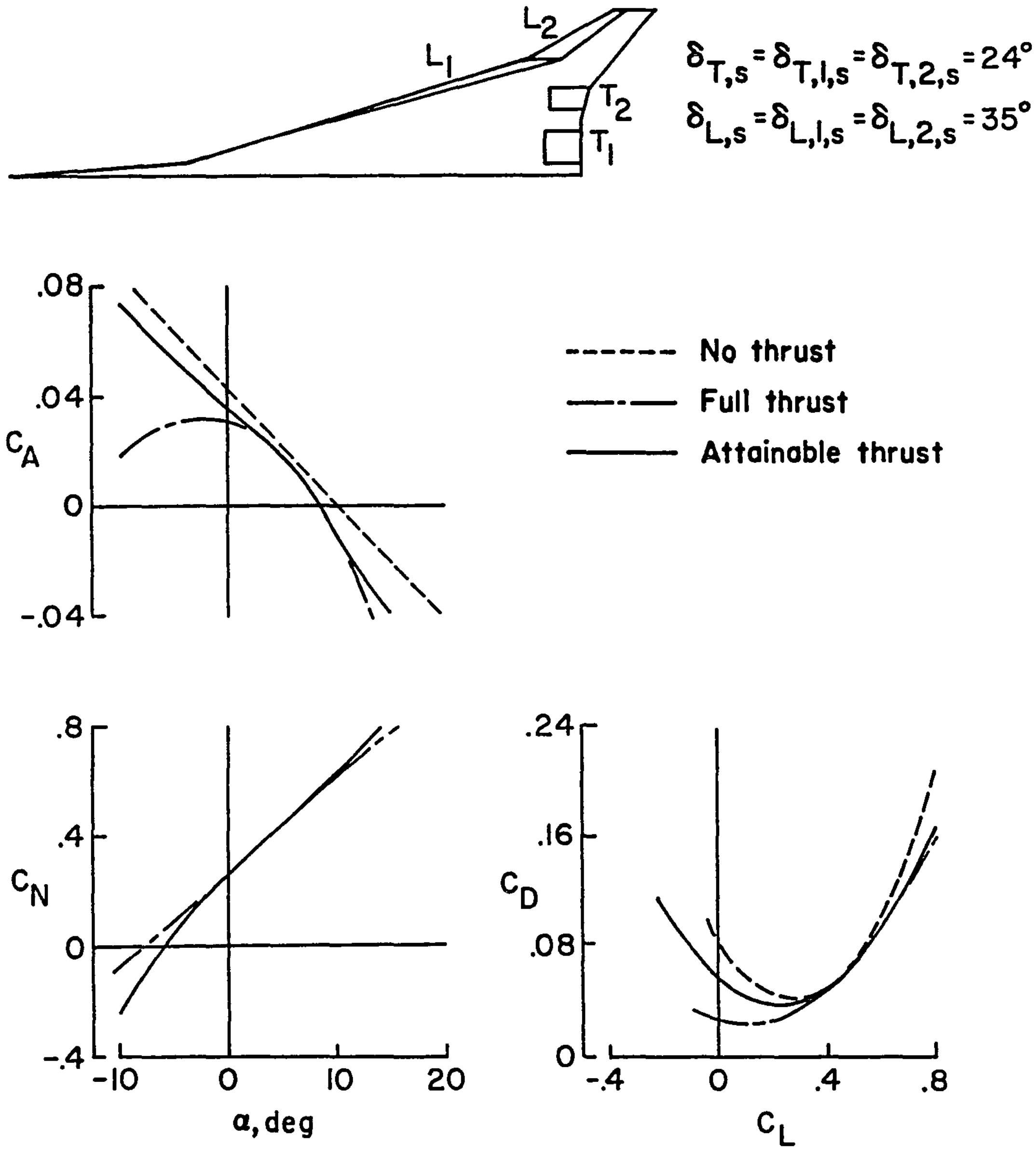

Figure 7. - Program aerodynamic forces for partial span leading edge flaps.

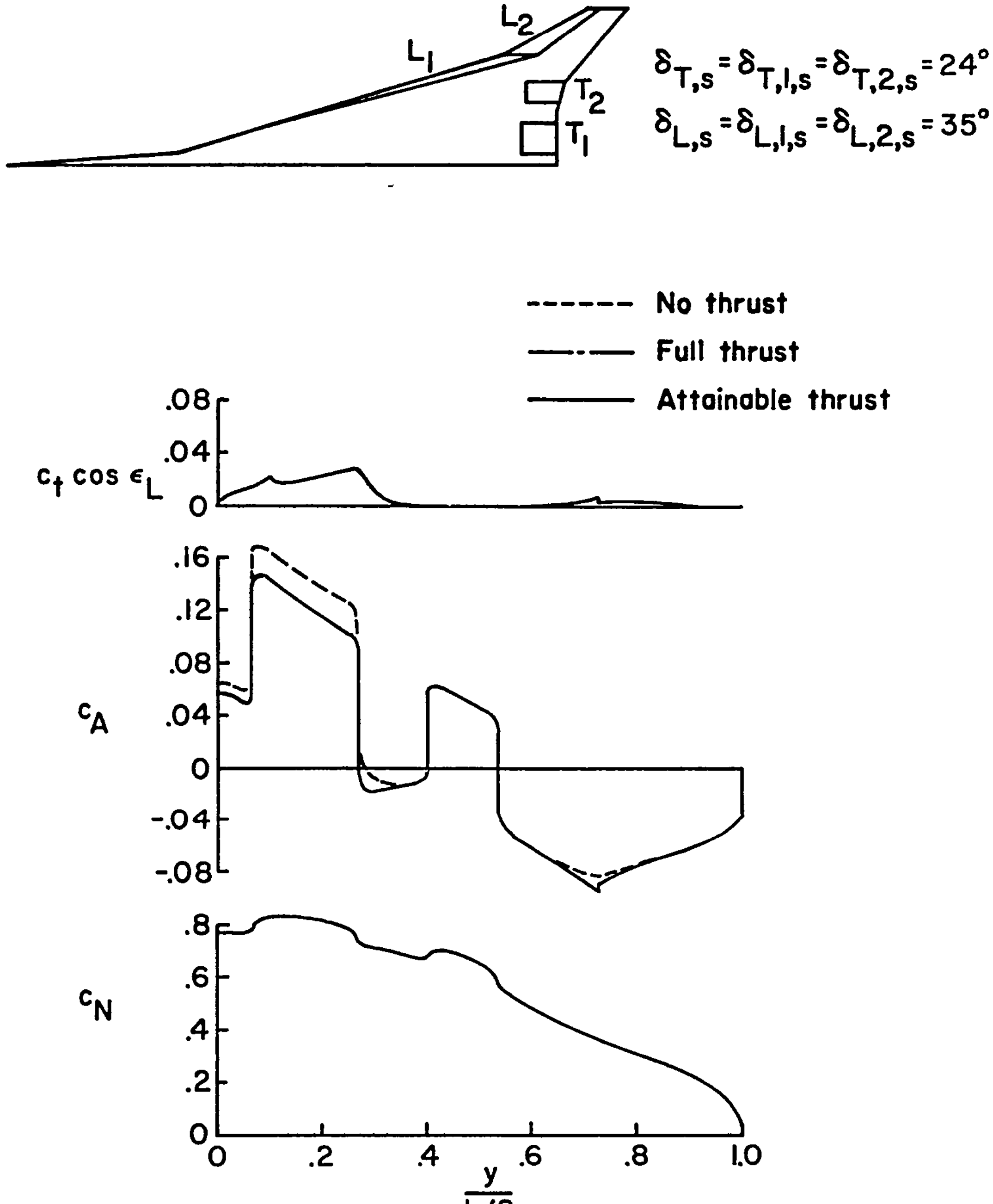

Figure 8. - Spanwise distribution of forces for partial span leading edge flaps at the design condition. C_L = .55. α = 8°.

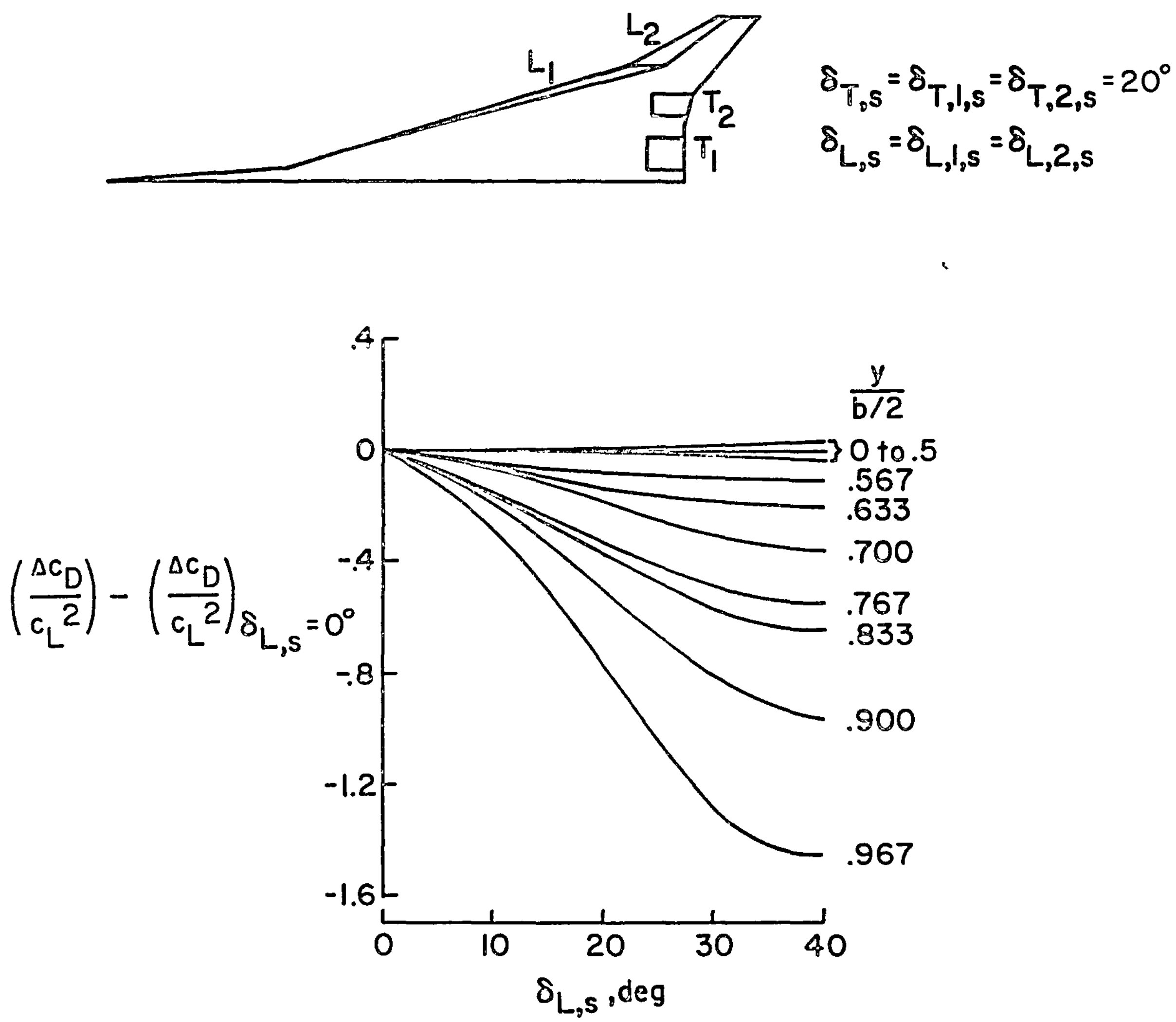

Figure 9. - Variation of section drag-due-to-lift factor with deflection of partial span leading edge flap system, $\alpha = 8°$.

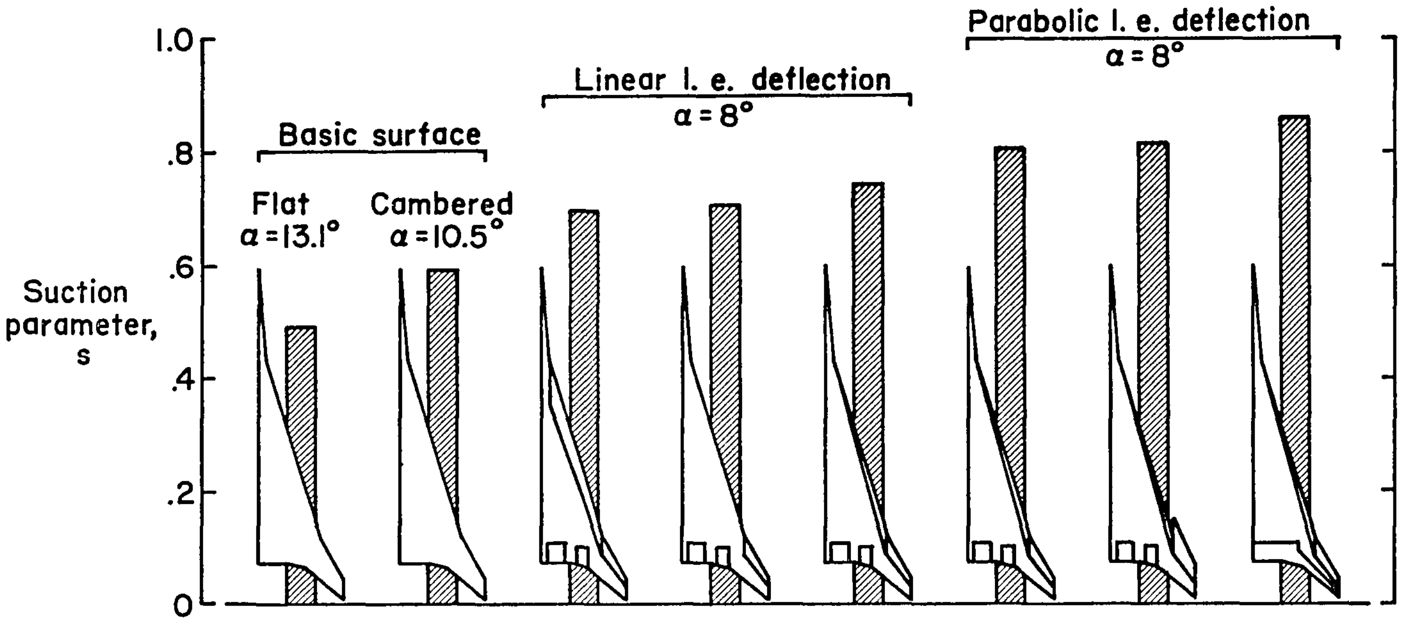

Figure 10. - Summary of suction parameters for the configurations studied. C_L = .55.

1 Report No	2 Government Accession No	3 Recipient's Catalog No
CR-165843		

4 Title and Subtitle
Application of an Aerodynamic Analysis Method Including Attainable Thrust Estimates to Low Speed Leading-Edge Flap Design for Supersonic Cruise Vehicles

5 Report Date
March 1982

6 Performing Organization Code

7 Author(s)
Harry W. Carlson

8 Performing Organization Report No

9 Performing Organization Name and Address
NASA Langley Research Center
Hampton, Virginia 23665

10 Work Unit No

11 Contract or Grant No
NAS1-16000

12 Sponsoring Agency Name and Address
National Aeronautics and Space Administration
Washington, DC 20546

13 Type of Report and Period Covered
Contractor Report

14 Sponsoring Agency Code

15 Supplementary Notes
Langley Technical Monitor - Samuel M. Dollyhigh

16 Abstract

A study of low speed leading-edge flap design for supersonic cruise vehicles has been conducted. Wings with flaps were analyzed with the aid of a newly developed subsonic wing program which provides estimates of attainable leading-edge thrust. Results indicate that the thrust actually attainable can have a significant influence on the design and that the resultant flaps can be smaller and simpler than those resulting from more conventional approaches.

17 Key Words (Suggested by Author(s))
Flap Design
Leading-Edge Thrust
Supersonic Cruise Vehicles

18 Distribution Statement
FEDD Restriction
UNCLASSIFIED - UNLIMITED
STAR CATEGORY 01

19 Security Classif (of this report)	20 Security Classif (of this page)	21 No of Pages	22 Price
Unclassified	Unclassified	28	A04

End of Document